

# Unmanned aerial vehicle design for disaster victim search and rescue operation using wireless sensor network localization

Fajar Sam Hutabarat, Imanuel Maurice Darmawan Sitanggang, Joy Andrew Immanuel Damanik, Guntur Petrus Boy Knight, Albert Sagala

Electrical Engineering, Institut Teknologi Del, Toba Samosir, Indonesia

## Article Info

### Article history:

Received Aug 1, 2022

Revised Sep 15, 2022

Accepted Oct 3, 2022

### Keywords:

Passive infrared

Search-and-rescue

Triangulation

Unmanned aerial vehicle

Victim search process

Website

## ABSTRACT

The search for disaster victims carried out by search-and-rescue (SAR) team mainly uses traditional methods, which are considered to take much time and effort, and pose a high risk for the search team and the victim. Based on this problem, we conducted research to assist disaster victim search. In this research, we designed a system using passive infrared (PIR) sensors to detect and measure the direction angle of the victim. Given the direction angle from different observation points' perspectives, we determine the victim's position using the triangulation method. We also designed a quadcopter unmanned aerial vehicle (UAV) to carry this sensor system across the disaster area. For monitoring purposes, a local website was designed to display data generated by the system. Based on test results, the system can determine a victim's position with a distance difference of less than 5 m. The system can search victim in an empty land  $\pm 35 \text{ m} \times 15 \text{ m}$  wide in 14 minutes 20 seconds. The data monitoring system also displayed the victim's position, the position of the observation points, and the UAV's flight path.

This is an open access article under the [CC BY-SA](#) license.



## Corresponding Author:

Albert Sagala

Electrical Engineering, Institut Teknologi Del

Toba Samosir, Indonesia

Email: albert@del.ac.id

## 1. INTRODUCTION

Search-and-rescue (SAR) is an activity carried out to find and save victims who are missing or who are feared missing due to an accident or disaster. Search activities are one of the main activities carried out by the SAR team [1]. The search process carried out by the SAR team often takes a lot of time and energy. Disaster areas also risk search teams and victims [2]. Time is the main determining factor of a victim's survivability in disaster events. Arnold *et al.* [3] described that the first 18 to 24 hours are the most critical time in a disaster. The victims' survivability could drop to 0% beyond 20 hours.

Based on these problems, we conducted this research to design a novel system that can assist the SAR team in finding and determining the position of disaster victim in a reasonably short time. This system used passive infrared (PIR) sensors to detect disaster victim. We also designed an unmanned aerial vehicle (UAV) to carry the sensor system through a disaster area. Based on the sensor's data from various surveillance points, the victim's position was determined using the triangulation method. These data were shown using a local monitoring website. This system has an advantage over other state-of-the-art systems in terms of processing time, as the sensor and method used were straightforward. The system is also designed to operate automatically. This research is also expected to be a reference for developing disaster victim search technology.

Most state-of-the-art SAR technologies use an unmanned aerial vehicle (UAV) system, which is equipped with a sensor system for detecting and determining human position. UAVs can significantly reduce

the search time for vast disaster areas [4]. Camera-equipped UAVs to detect and determine the victim's position had been utilized. Lee *et al.* [4] used infrared camera because the system is intended to search disaster victim in a large dark room. Erdos *et al.* [5] utilized a commercially available fixed-wing UAV (UAV which generates lift from their wings, such as airplanes). In contrast, the other two references used a rotary-wing UAV (UAV which generates lift from their propellers, such as helicopters, quadcopters, and hexacopters). The system in [4] and [5] still relied on the operator for detecting the victim, but the system in [6] was capable of detecting and determining the victim's position automatically using an image processing algorithm.

Serrano [7] utilized a quadcopter UAV with a thermal camera to detect and determine the victim's position. The UAV also has a standard camera to map the disaster area. The system detects victims and maps the disaster area using an image processing algorithm. The victims' positions are shown on the generated map.

More than one UAV that works together had been utilized, thus shortening the victim search and positioning process even further. Auer *et al.* [8] used several rotary-wing UAVs equipped with a camera so that operators could see a live view of the state of the disaster area. One of the UAVs is also equipped with a ground-penetrating radar (GPR) sensor, allowing it to search for victims buried under the rubble. Kobayashi *et al.* [9] used multiple rotary-wing UAVs equipped with ultra-wide band (UWB) radio modules. The radio modules form a communication network, thus enabling each UAV to communicate and work together to find the victim. As it is assumed that the victim used a device capable of communicating with the UAV's radio module, the victim's position can be determined using the localization method.

Unlike previous references, land-based vehicles equipped with sensors were also used to detect and determine the victim's position [10]–[12]. Ground-based vehicles are used because this research aims to determine the position of victims who are in tight spaces or crushed by debris, so UAVs are not up for the task. In addition, the three references used a thermal camera; thus, the detection and positioning of the victim were also carried out using an image processing algorithm.

## 2. RESEARCH METHOD

This section describes the system design used in this research. First, the system is modeled using block diagram. Then, the data flow from sensor readings to system operators is described. The UAV system design is then discussed based on the sensor system. After that, the method of determining the victim's position used in this study is described. Lastly, the data monitoring system is then discussed based on the assumption of the disaster area condition.

### 2.1. System overview

Figure 1 shows the block diagram of the entire system used in this research. The UAV system consists of a radio, sensor, control, propulsion, and power supply system. The sensor system consists of a data processing system and HC-SR501 PIR sensors. The reason for using PIR sensors will be discussed in the following subsection. The operator's computer is modelled as a data monitoring system. The sensor system gets power through the UAV's power supply system. The sensor system can communicate with the UAV control system to obtain the whole system's position data. The sensor system can also communicate with the operator's computer through a wireless local area network (WLAN).

Figure 2 shows the data flow from the sensor system to the operator. First, the data taken by PIR sensors will be processed by the processor to become helpful information for the search process, such as the total detection of each sensor, the direction angle of the detected victim, and the victim's position. The data were then stored inside a database and displayed on a website by the web server. Finally, the operator observes the data through their web browser.

### 2.2. Sensor system design

Human detection can be done based on human characteristics (such as movement, size, and body temperature) or based on objects carried by the human (such as smartphones, and radio frequency identification/RFID) [13]. Human detection based on human characteristics is referred device-free, and detection based on objects carried by humans is referred device-based [14]. This research assumes that the victim's device, such as a smartphone, is not with the victim or the device is inactive, so victim detection must rely on human characteristics (device-free).

There is also a possibility that the victim is trapped inside rubble, so the used sensor must be able to penetrate the rubble [15]. However, this research is limited to detecting a victim whose position is on the surface of the disaster area, so the sensors used do not need to be able to penetrate the debris material. Based on the given assumption and limitation, several sensors are appropriate for this human detection problem, such as cameras, thermal cameras, PIR sensors, microphones, ultrasonic sensors, radar, and CO<sub>2</sub> sensors [13]. In this research, the authors are interested in using PIR sensors to detect and determine the victim's position.

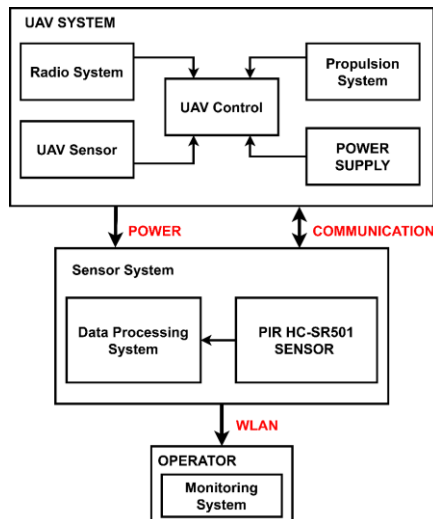


Figure 1. System block diagram

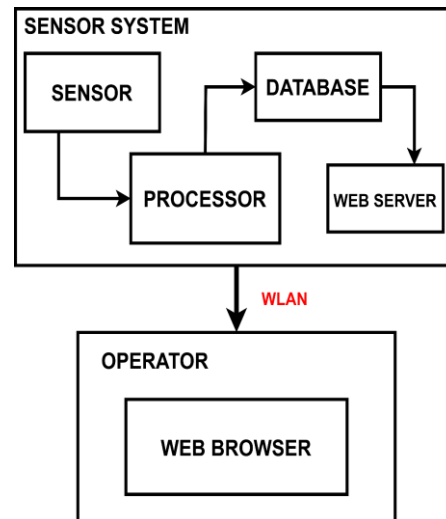


Figure 2. Data flow diagram between sensor system and operator

The PIR sensor is a motion sensor that can detect changes in the amount of infrared radiation in its field of view (FOV) [16]. One type of PIR sensor that is commonly used is the HC-SR501 sensor. Based on the datasheet [17], this sensor consists of one PIR sensor element and an integrated circuit (IC). The change in the amount of infrared radiation observed by the PIR sensor element (in the form of an analogue signal) is then converted into a digital signal ('0' and '1' signal) by the IC. Thus, PIR sensor detects the presence of movement in its field of view. This research assumes that the victim can move (without displacement), thus, enabling the PIR sensor to detect the victim. Furthermore, this research also assumes that there are no other sources of movement in the disaster area beside the victim. Thus, the movement detected by the PIR sensor can be interpreted as the victim's movement.

Until this part, the problem of detecting the victim has been solved using PIR sensor. The next part is to solve the problem of determining the victim's position using the PIR sensor. Some literature shows that analogue and digital signals of PIR sensors can determine human position. We can obtain the analogue signal of a PIR sensor by using its element directly. The human's position is determined by analyzing the signal. On the other hand, determining human position using PIR sensor's digital signal generally requires several PIR sensors, either arranged as a single unit or scattered in several places [18].

Digital signals from PIR sensors to determine human location had been used. Yuebin *et al.* [19] used several PIR sensors arranged in the form of a rack so that it can determine the human's direction angle. The sensor system is placed on a wheeled robot, allowing it to measure the direction angle of the human from different reference points. The human position can then be determined based on these data. Lai *et al.* [20] focused on the use of PIR sensors inside a room. The sensor system is packed with several PIR sensors placed on the ceiling, thus enabling it to detect and determine the location of a human. Lee *et al.* [21] also used several PIR sensors placed on the ceiling, but the sensors were spread apart at several points.

Analog signals from PIR sensors had been used to determine human location. Narayana *et al.* [18] had investigated the characteristics of the PIR sensor's analogue signal generated by humans at different distances and moving speeds. Using some of his sensor systems, the author successfully determined the human's position. Zhang *et al.* [22] used eight sensor systems spread throughout the room. Each sensor system has four sensor elements which can detect nine different areas so that the direction of human movement can be determined. Liu *et al.* [23] investigated a method that can determine the human position more accurately.

This research used the digital signal of the PIR sensor because it is simpler and can be processed with small computational costs. Furthermore, only the sensor system from Yuebin *et al.* [19] can change position (mobile sensor). In the event of a disaster, it may not be feasible to install the sensor system in a fixed position; thus, the sensor system must be able to move through the disaster area. The designed sensor system is also more straightforward than those designed by other references. Based on these considerations, we choose to utilize this designed sensor system to detect and determine the position of victims in disasters.

Figure 3 shows the design of the sensor system used in this research in 3D view Figure 3(a) and top view Figure 3(b). Our sensor system consists of 10 HC-SR501 PIR sensors arranged in a circle. In this research, we use HC-SR501 PIR because it is often used and has a relatively low cost. The circular

arrangement of the PIR sensors allows the sensor system to detect the victim around it ( $360^\circ$ ). In Figure 3(a), it is shown that each PIR sensor is tilted slightly downwards; thus, the PIR sensors can observe the surface of the disaster area. The tilt angle is  $45^\circ$ , so the PIR sensors can detect up to its farthest point. In Figure 3(b), it is shown that there was a gap in front of each PIR sensor. This gap limits the sensor's field of view (initially  $110^\circ$  [17]) so that each PIR sensor only observes a predetermined sector. This gap measures  $36^\circ$ , so with 10 PIR sensors, the total angle the sensor system covers are  $360^\circ$ . Raspberry Pi 4 is used for processing, storing, and displaying data.

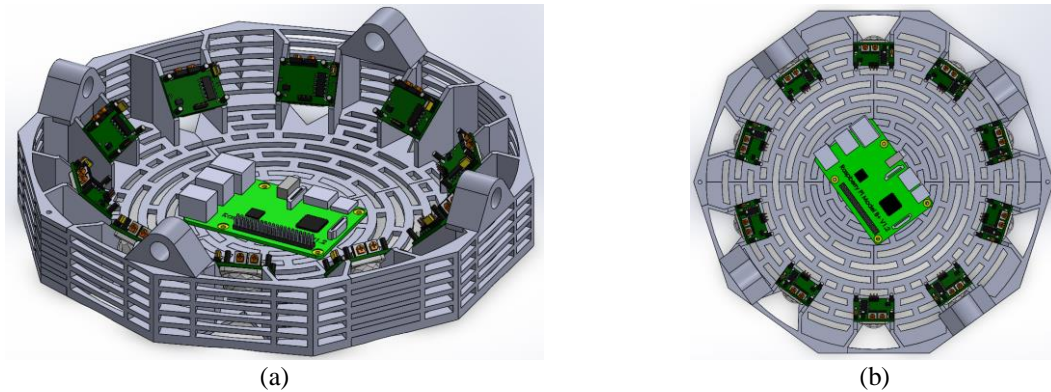


Figure 3. Design of the sensor system along with its components in (a) 3D view and (b) top view

Figure 4 describes the top view of the sensor system along with its detection area. The circle around the sensor system describes the detection area of the sensor system. The size of the circle has not been scaled to the detection range of the sensor system. The cells labelled C1, C2, up to C10 are detection cells for the PIR1, PIR2, up to PIR10 sensors, respectively. Each PIR sensor can only observe the disaster area in its given detection cell. Since there are 10 PIR sensors, each detection cell measures  $36^\circ$ . The cells are arranged from a  $0^\circ$  angle and continued counterclockwise until returning to the starting angle.

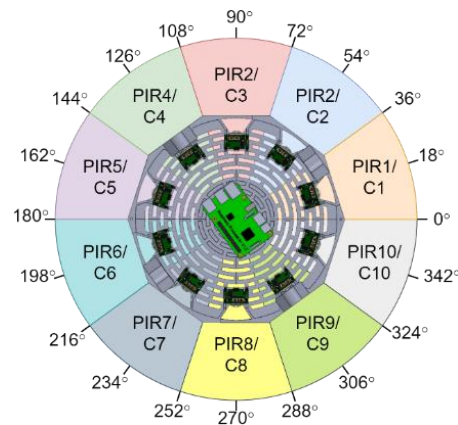


Figure 4. The top view of the sensor system along with its detection area

For example, PIR1 can only observe the disaster area at an angle range of  $0^\circ$  to  $36^\circ$ , PIR2 can only observe the disaster area at an angle range of  $36^\circ$  to  $72^\circ$ , and so on. If one of the PIR sensors detects movement from the victim, it can be inferred that the victim is in its range of detection. The actual direction angle of the victim can be anywhere within that range, but because the PIR sensor can only give digital signals ('0' and '1'), the direction angle of the victim cannot be determined with a continuous value. We chose to approximate the direction angle of the victim using the direction angle of the PIR sensor because we can assume that the victim is right in front of the sensor. The direction angle of the PIR sensor is taken from the center angle of the PIR sensor's detection angle range.

Figure 5 illustrates two example scenarios of victim detection. First, the victim's whole body is in PIR1's detection cell in Figure 5(a). Next, the victim's body is between PIR6's and PIR7's detection cells in Figure 5(b).

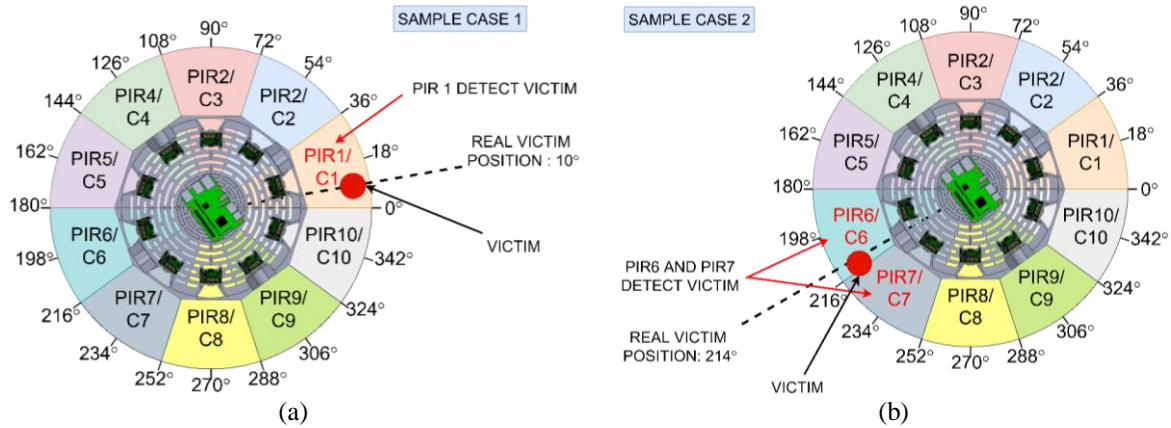


Figure 5. Two example scenarios of victim detection, the victim being in (a) PIR1's detection cell and (b) PIR6's and PIR7's detection cell

For the example scenario in Figure 5(a), let us assume that the actual direction angle of the victim is  $10^\circ$ . The direction angle of the victim is in PIR1's detection angle range (i.e.  $0^\circ$  to  $36^\circ$ ); thus, PIR1 detects the victim (PIR1 issues signal '1'). Because PIR1 is facing towards an  $18^\circ$  angle (the center angle of  $0^\circ$  to  $36^\circ$  angle range is  $18^\circ$ ), the sensor system will conclude that there is a victim in front of PIR1; thus, it will assume that the victim is at direction angle of  $18^\circ$ .

For the example scenario in Figure 5(b), let us assume that the actual direction angle of the victim is  $214^\circ$ . PIR6 and PIR7 will both detect the victim. PIR6 is facing toward  $198^\circ$  angle, while the PIR7 is facing toward  $234^\circ$ . The sensor system will conclude that the victim is in the middle of PIR6 and PIR7; thus, it will assume that the victim is at a direction angle of  $216^\circ$  (the center angle of PIR6 and PIR7).

We are aware that there is a fairly significant error in the process of approximating the direction angle of the victim. But we did not solve this problem as a unique method is required so that the approximation is correct. This problem needs to be solved in future research.

Figure 6 shows the sensor system's detection area when viewed by the ground and top observer in front of the system in Figure 6(a) and behind the system in Figure 6(b). We assume there is a victim in PIR4's detection cell for reference. In this figure, the sensor system is airborne. We will explain the figure based on the points included.

In Figure 6(a), point 1 shows the sensor system and UAV in the air. Point 2 shows the sensor system when viewed closely from the front. According to the observer on the ground, PIR1 is on the far left, followed by PIR2, PIR3, PIR4, and PIR5. Other PIR sensors are located at the back; thus, the observer cannot see them. Detection cells of each PIR sensor are depicted in the same color as in Figure 4. Point 3 illustrates an example victim. Point 4 shows the top view of the sensor system. The PIR6 to PIR10 detection areas are darkened to indicate that the observer cannot see the PIR sensor's detection area from the front. The victim (Point 3) appears as if it was covered by the detection cell of PIR4.

In Figure 6(b), point 1 shows the sensor system and UAV in the air. Point 2 shows the sensor system when viewed closely from the back. According to the observer on the ground, PIR6 is on the far left, followed by PIR7, PIR8, PIR9, and PIR10. Other PIR sensors are located at the front; thus, the observer cannot see them. Detection cells of each PIR sensor are depicted in the same color as in Figure 4. Point 3 illustrates the position of the previous example victim. Point 4 shows the top view of the sensor system. PIR1 to PIR5 detection areas are darkened to indicate that the observer cannot see the PIR sensor's detection area from behind. The victim is no longer visible in the image because the victim is in front.

Figure 6 also shows that the altitude of the UAV ( $h$ ) will affect the detection radius of the sensor system ( $r$ ). Based on simple geometric calculations, it can be inferred that:

$$\tan 45^\circ = \frac{h}{r} \quad (1)$$

$$h = r$$



In other words, when the UAV flies at an altitude of 10 m, the detection radius of the sensor system is also 10 m. However, due to the maximum distance of the PIR sensor used being 7 m [17], then the height of the UAV of more than 5 m will render the PIR sensor unable to observe the area. Therefore, in this research, the UAV flew at an altitude of 5 m when the sensor system was active.

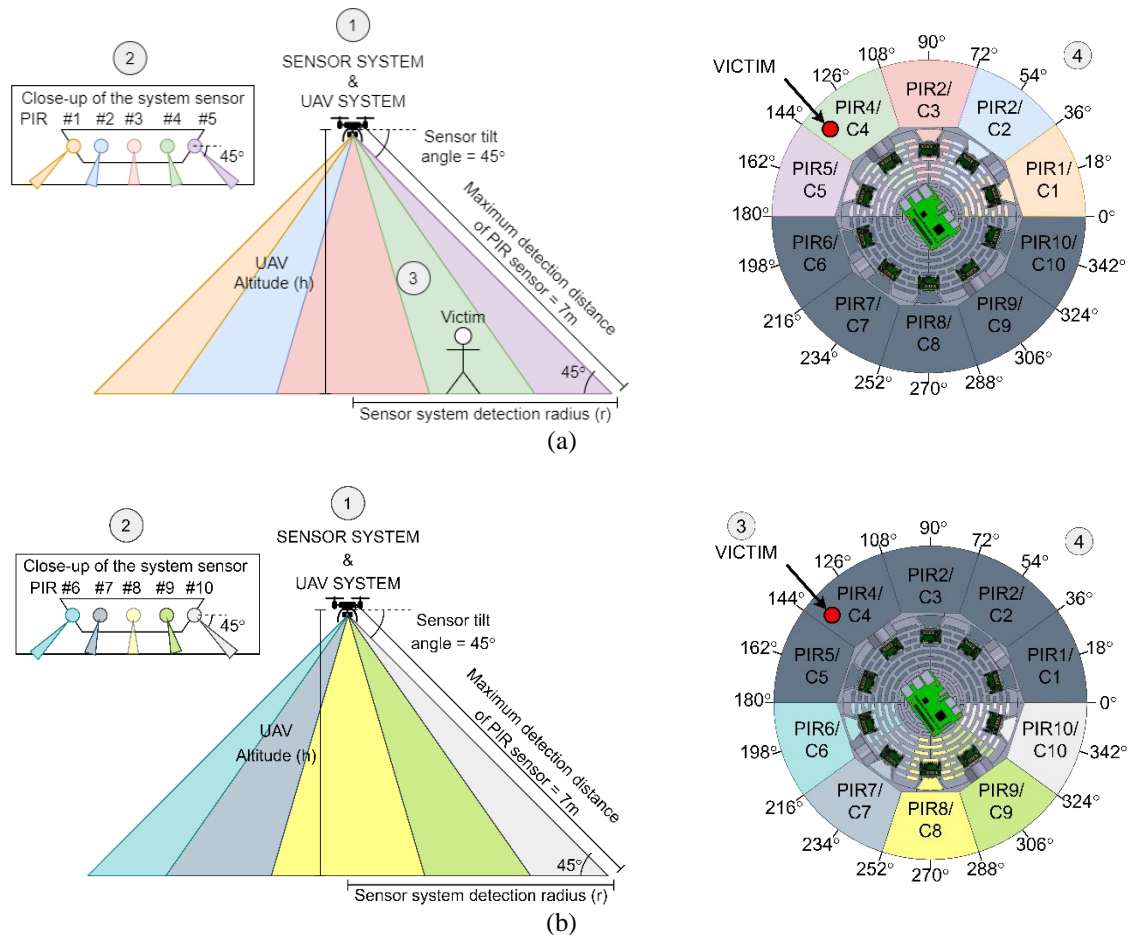


Figure 6. Sensor system's detection area when viewed by ground and top observer (a) in front of the system and (b) behind the system.

### 2.3. UAV system design

The sensor system needs transportation media that can be used to help it navigate through a disaster area. Transportation media can generally be divided into land-based, sea-based, and air-based. This study assumes disaster areas such as earthquakes, landslides, or unnatural disasters, so sea-based transportation is impossible to use. On the other hand, land transportation media may have difficulty passing through disaster areas, so the only option is air-based transportation. Therefore, we designed a UAV as the transportation media of the described sensor system. The UAV is designed to support the sensor system in making observations at several points in the disaster area. For this reason, the UAV must be able to stay in the air steadily (hovering) when the sensor system takes data at the observation points.

UAVs are divided into two types: fixed-wing [24] and rotary-wing [8]. The type that is generally used for hovering purposes is rotary-wing UAVs because it uses propellers to stay in the air [4], [6]–[8], [24]. Therefore, this research was conducted using a commonly used type of rotary-wing UAV, a quadcopter (UAV with four propellers). Quadcopter arm configuration can be plus (+) or cross (×) configuration [25], [26]. The cross configuration (×) is capable of lifting more loads, as well as being more stable and appropriate for hovering applications [25], [26]; thus, this arm configuration was used in this study.

The UAV's propulsion system uses four T-Motor MN3510-15 630 KV brushless DC motors, four 15" \* 5.5" propellers, Cyclone XF 35A 4-in-1 ESC, and a Li-Po 6S 6200 mAh battery. This motor and propeller combination can produce thrust up to 2kg. When using all four, the maximum thrust produced by

the UAV is 8 kg. Ononiwu *et al.* [25] mentioned that the rule of thumb for the UAV to take off easily and have a good control response is to limit the weight of the UAV to half of the maximum thrust produced by the UAV, so the maximum weight of the UAV is 4 kg. The implemented UAV weights 2 kg, much lighter than the maximum weight value.

UAV's control system includes Matek H743 mini flight controller (FC), Ublox NEO M8N GPS sensor, FS-I6 & FS-IA10 remote control (R/C) transceiver, 3DR radio 433MHz telemetry module, HD 700TVL FPV camera, and AKK FX3 ultimate video transmitter. These components were selected by considering their compatibility with UAV's open-source firmware, Ardupilot. Figure 7 shows the 3D design of the whole system in Figure 7(a) and the actual implementation of the system in Figure 7(b). It can be seen that the sensor system is placed at the bottom of the UAV system.



Figure 7. Images showing (a) the 3D design of the whole system and (b) the actual implementation of the system

Figure 8 shows an overview of the PIR sensor arrangement referenced to the UAV system. The UAV's head is facing north. The  $0^\circ$  angle of the sensor system is positioned on the UAV's east side. The UAV's direction must be considered when processing the observation data of the disaster area because the sensor system only determines the direction angle of the victim relative to the UAV. Therefore, the reference of the direction angle needs to be changed from UAV reference to global reference ( $0^\circ$  in the north,  $90^\circ$  in the east) so that the Triangulation process will produce correct data.

Figure 9 shows the direction angle of the victim on global reference for the  $i$ -th observation point. The UAV's direction angle is  $\theta_{UAV,i}$ , The direction angle of the victim on the UAV reference is  $\theta_{victim,i}$ , and the direction angle of the victim on the global reference is  $\theta_i$ .  $\theta_i$  can be calculated as (2).

$$\theta_i = \theta_{UAV,i} + 90^\circ - \theta_{victim,i} \quad (2)$$

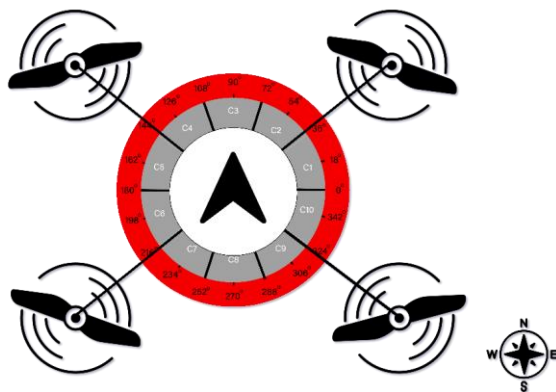


Figure 8. An overview of the sensor arrangement with UAV as reference

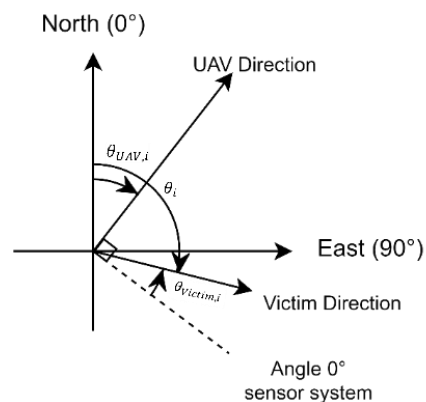


Figure 9. Depiction of the victim's direction angle on the global reference for the  $i^{\text{th}}$  observation point

The UAV (together with the sensor system) is designed to navigate through the disaster area and observe the victim's movement from different observation points. These observation points, of course, need to be arranged in such a way so that the sensor system can observe the entire disaster area. The method of arranging observation points used in this research is described in Figure 10. The disaster area to be observed is depicted as a rectangle with length  $p$  and width  $l$ . The black dot in the image represents the observation point, while the blue circle around it represents the detection radius of the sensor system.

The arrangement of the observation points is obtained by setting the distance between the observation points to be  $\sqrt{3}r$  with  $r$  as the sensor's detection radius as shown in Figure 11. Liao *et al.* [27] mentioned that this distance could maximize the coverage area of the sensor system. As previously discussed, the UAV will only fly at an altitude of 5 m when it is hovering at the observation point, so the detection radius of the sensor is 5 m, and the distance between the observation points must be  $5\sqrt{3}m = 8.66m$ .

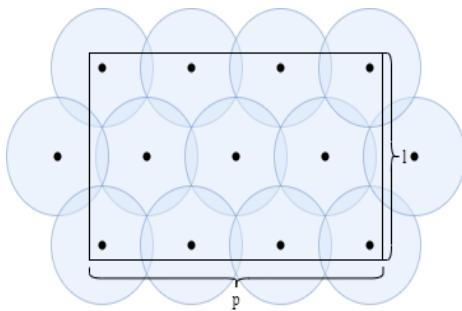


Figure 10. The arrangement of observation points used in this research

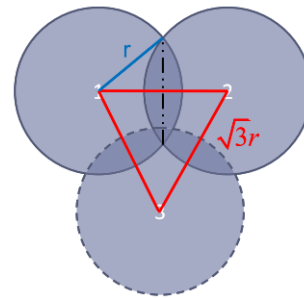


Figure 11. Arrangement of three circles, each separated with a distance of  $\sqrt{3}r$  (Source [27])

After the observation points have been successfully arranged and determined, the UAV goes through these points individually. Figure 12 shows various UAV flight paths that can be used for searching the disaster victims. A more detailed explanation can be seen in [28]. This research is carried out using parallel track search. This flight path is implemented by traversing the observation points line by line.

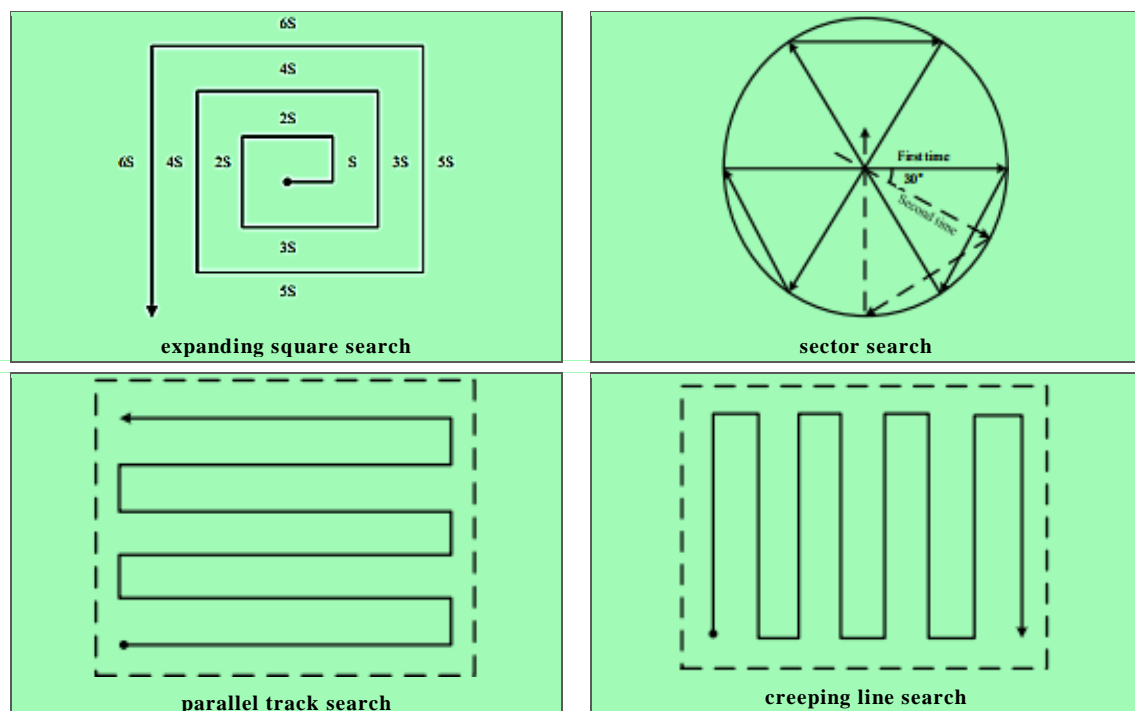


Figure 12. Various forms of UAV flight paths for the victim search process [28]



## 2.4. Localization

Based on the previous literature review, only Kobayashi *et al.* [9] uses localization method. Therefore, the method of determining the victim's position in this research is closely related to the method used in that research. Localization is defined as the process of determining the position of an object. This process begins by taking data related to the object's position based on several reference points and then calculating the object's position based on that data [29].

Data related to an object's position can be in the form of distance between the object and the reference points, such as time of arrival (TOA), time difference of arrival (TDOA), round trip time (RTT) and received signal strength (RSS). The data can also be the object's direction angle based on reference points, such as the angle of arrival (AOA). The position of the object can then be calculated using trilateration (calculating the object's position based on distance data) or triangulation (calculating the object's position based on angle data) [29]. Zhang *et al.* [29] also mentioned that the optimization process is commonly done to improve the accuracy of the calculation.

TOA concludes the distance between the object and the reference point by calculating the time it takes for the signal to propagate from the object to the reference point. TDOA uses two signals with different propagation velocities and then compares the arrival time between the two. RTT infers the distance by calculating the time it takes for the signal to propagate from the reference point to the object and back. RSS relies on the object's signal strength at the reference point. AOA relies on the direction angle of the signal from the object [29].

Trilateration can determine the victim's position based on the distance data between the object and the reference point [29]. Figure 13 shows the process of determining object  $T$ 's position based on three reference points:  $A(x_1, y_1)$ ,  $B(x_2, y_2)$ , and  $C(x_3, y_3)$ . The distance between the object to each reference point, which may be obtained through TOA, TDOA, RTT, or RSS technique, are  $R_1$ ,  $R_2$ , and  $R_3$ . Each reference point forms a circle equation, which can be merged into a system of equations as (3),

$$\begin{cases} (x_1 - x)^2 + (y_1 - y)^2 = R_1^2 \\ (x_2 - x)^2 + (y_2 - y)^2 = R_2^2 \\ (x_3 - x)^2 + (y_3 - y)^2 = R_3^2 \end{cases} \quad (3)$$

where  $(x, y)$  is the unknown position of object  $T$  [29]. When there are  $n$  reference point, the system of equations becomes (4).

$$\begin{cases} (x_1 - x)^2 + (y_1 - y)^2 = R_1^2 \\ (x_2 - x)^2 + (y_2 - y)^2 = R_2^2 \\ \vdots \\ (x_n - x)^2 + (y_n - y)^2 = R_n^2 \end{cases} \quad (4)$$

Triangulation can determine the victim's position based on the direction angle data between the object and the reference point [29]. Figure 14 shows the process of determining object  $X$ 's position based on three reference points:  $L_1(x_1, y_1)$ ,  $L_2(x_2, y_2)$ , and  $L_3(x_3, y_3)$ . The direction angles of the signal (which is referenced to a particular direction, such as the  $x$ -axis or north direction) from object  $X$  to each reference point (obtained from the AOA technique) are  $\theta_1$ ,  $\theta_2$ , and  $\theta_3$ . Each reference point forms a line equation, which can be merged into a system of equations as (5),

$$\begin{cases} Y - y_1 = (X - x_1) \tan \theta_1 \\ Y - y_2 = (X - x_2) \tan \theta_2 \\ Y - y_3 = (X - x_3) \tan \theta_3 \end{cases} \quad (5)$$

where  $(X, Y)$  is the unknown position of object  $X$ . When there are  $n$  reference point, the system of equations become (6).

$$\begin{cases} Y - y_1 = (X - x_1) \tan \theta_1 \\ Y - y_2 = (X - x_2) \tan \theta_2 \\ \vdots \\ Y - y_n = (X - x_n) \tan \theta_n \end{cases} \quad (6)$$

The equations formed by trilateration and triangulation can be solved by the least-square approach [30]. The system of equations of the two methods, namely (4) and (6), can be written simply as (7).

$$A \mathbf{c}^T = \mathbf{b} \quad (7)$$

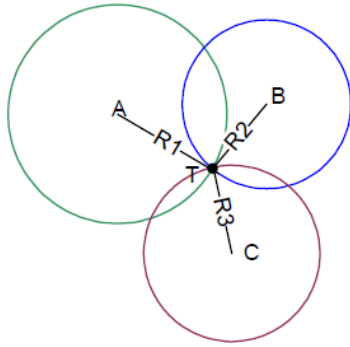


Figure 13. Trilateration using three reference points [29]

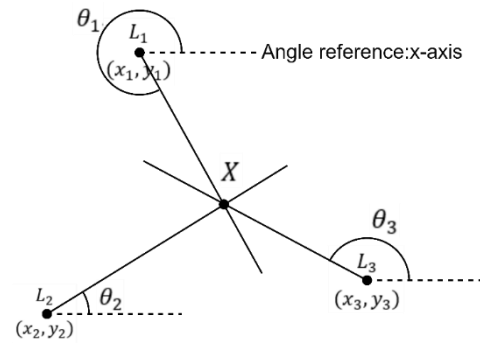


Figure 14. Triangulation using three reference points

For trilateration (4), the value of  $\mathbf{A}$ ,  $\mathbf{c}$ , and  $\mathbf{b}$  is shown in (8). These values are obtained by subtracting each equation from the previous equation and then rearranging the system of equations so that it can be simplified as matrix (7) [29].

$$\mathbf{A} = \begin{bmatrix} 2(x_1 - x_n) & 2(y_1 - y_n) \\ \vdots & \vdots \\ 2(x_{n-1} - x_n) & 2(y_{n-1} - y_n) \end{bmatrix}$$

$$\mathbf{c} = [x \quad y]$$

$$\mathbf{b} = \begin{bmatrix} x_1^2 - x_n^2 + y_1^2 - y_n^2 + R_n^2 - R_1^2 \\ \vdots \\ x_{n-1}^2 - x_n^2 + y_{n-1}^2 - y_n^2 + R_n^2 - R_1^2 \end{bmatrix}$$
(8)

For triangulation (6), the value of  $\mathbf{A}$ ,  $\mathbf{c}$ , and  $\mathbf{b}$  is shown in (9). Just like trilateration, these values are obtained by rearranging the system of equations so that it can be simplified as matrix (7) [30].

$$\mathbf{A} = \begin{bmatrix} -\tan \theta_1 & 1 \\ -\tan \theta_2 & 1 \\ \vdots & \vdots \\ -\tan \theta_3 & 1 \end{bmatrix}$$

$$\mathbf{c} = [X \quad Y]$$

$$\mathbf{b} = \begin{bmatrix} y_1 - x_1 \tan \theta_1 \\ y_2 - x_2 \tan \theta_2 \\ \vdots \\ y_n - x_n \tan \theta_n \end{bmatrix}$$
(9)

Matrix (7) can then be solved to determine the position of the object:

$$\mathbf{A} \mathbf{c}^T = \mathbf{b}$$

$$\mathbf{A}^{-1} \mathbf{A} \mathbf{c}^T = \mathbf{A}^{-1} \mathbf{b}$$

$$\mathbf{c} = ((\mathbf{A}^T \mathbf{A})^{-1} \mathbf{A}^T \mathbf{b})^T$$
(10)

The sensor system generates direction angle data of the victim; thus, the sensor system can be considered to calculate the victim's AOA value from observation points (reference points). As previously stated, using Triangulation, the object's position can be calculated based on AOA values. In this research, the direction angles of the victim based on observation points (2) were arranged as (6). The equations were solved using the least-square approach (7), (9), and (10) to determine the victim's position. The position of the victim generated by this method is not optimized due to the limitations of the designed PIR sensor system. The resulting victim's position needs to be optimized in future research, thus increasing its accuracy.

### 2.5. Data monitoring system

This research assumes that the internet service does not work in the disaster area, so the data exchange from the monitoring system to the operator is carried out using a wireless local area network (WLAN). The sensor systems and operator's computer will be connected via IEEE 802.11 (Wi-Fi) standards. The operator can monitor the data from the sensor system through its website. On the monitoring website, there are data generated by the sensor system at each observation point, the position of the victim (in longitude and latitude), and the UAV's flight path.

## 3. RESULTS AND DISCUSSION

This section will discuss the experimental scenario done in this research. The results of the experiment will be discussed in the following subsection.

### 3.1. System test scenario

The system is tested with a scenario where one victim is placed at a random position in an empty land. The victim will move his body on the spot. Figure 1 shows the experimental scenario carried out in this research. The 12 observation points were positioned manually by the operator, with an arrangement as previously described (the distance between points is 8.66 m). This arrangement enables the system to observe an area of  $\pm 35 \times 15$  m. The system then traverses the land automatically, moving from one observation point to another, using parallel track search flight path. The sensor system observed the point for 60 seconds. After the system traverses the area, the data generated by the sensor system at each observation point, the position of the victim generated by the triangulation process, and the data displayed by the data monitoring system will be observed.

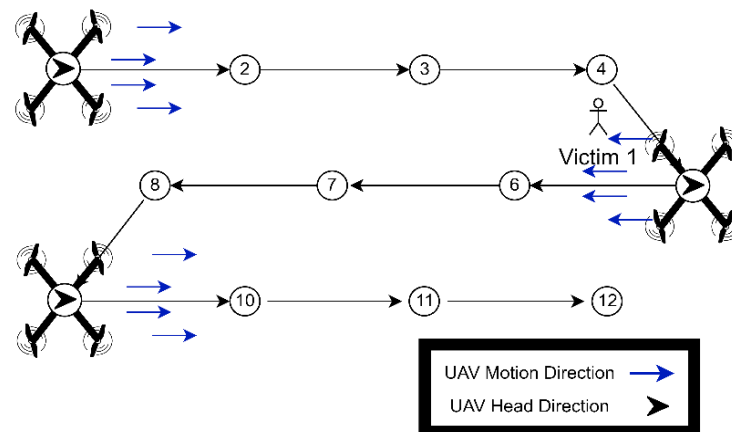


Figure 1. System test scenario

### 3.2. Test result

This experimental scenario was carried out in the green field of Del Institute of Technology campus. The weather was partly sunny with a reasonably weak wind force. Figure 16 shows the waypoints (observation points), which are planned using Mission Planner. Table 1 shows the longitude and latitude position of each waypoint.

The time required by the system to complete this experimental scenario is 14 minutes and 20 seconds. In detail, the UAV took off to a height of 5 m at the home point for 10 seconds, moving to the first observation point for 5 seconds, observing it for 60 seconds, and then moving to the second point for 10 seconds, and so on up until the last point. There are 12 observation points; thus, the system spent  $12 \times 60$  seconds = 12 minutes observing each point. The system spent  $11 \times 10$  seconds = 1 minute 50 seconds when traversing all the waypoints. The system lands on the spot for 15 seconds at the last point.

The battery is fully charged when the experiment is performed. After the experiment was complete, we observed that the remaining battery of the UAV was 30%. This value is the minimum percentage of the UAV's battery when in use. If the UAV is used more than that, then the failsafe system of the UAV will turn on and cancel the victim search mission. This also shows that the UAV flight time needs to be further increased so that the search process can be carried out longer and broader.

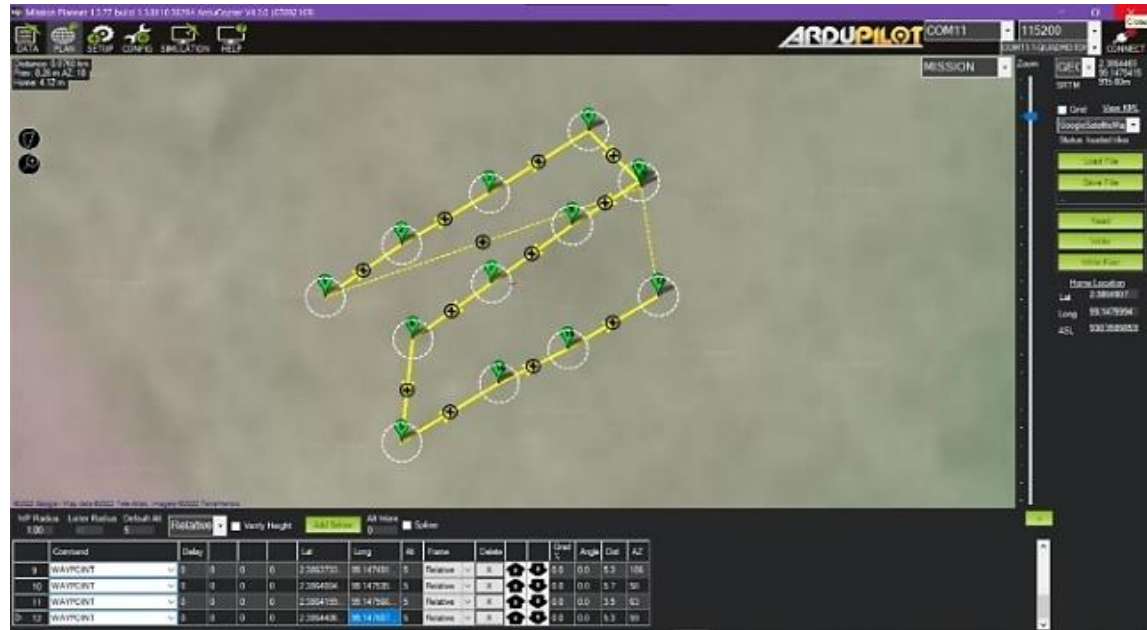


Figure 16. Waypoint planning in the mission planner

Table 1. UAV's position and heading direction at each observation point

Waypoint	Waypoint Position		UAV direction angle (°)
	Longitude	Latitude	
Waypoint-1	99.147356	2.386440	64.629780
Waypoint-2	99.147491	2.386464	62.209315
Waypoint-3	99.147530	2.386488	61.375122
Waypoint-4	99.147575	2.386516	71.276904
Waypoint-5	99.147598	2.386493	63.519874
Waypoint-6	99.147568	2.386473	61.343103
Waypoint-7	99.147531	2.386446	60.951332
Waypoint-8	99.147496	2.386420	60.821851
Waypoint-9	99.147491	2.386373	62.073639
Waypoint-10	99.147535	2.386400	67.480515
Waypoint-11	99.147566	2.386415	52.396283
Waypoint-12	99.147607	2.386440	48.943417

The data generated by the sensor system at each observation point can be seen in Table 2. The second column of Table 2 shows the total detection count of each PIR sensor for 60 seconds of observation. The data is arranged, starting from the total detection of PIR1, PIR2, up to PIR10.

Table 2. Total detections count of each PIR sensor

Waypoint	Total detection count of each PIR sensor	PIR sensors that detect the victim
Waypoint-1	[0, 0, 0, 0, 0, 0, 0, 0, 0, 0]	None
Waypoint-2	[0, 0, 0, 0, 0, 0, 0, 0, 0, 0]	None
Waypoint-3	[0, 0, 0, 0, 0, 0, 0, 0, 0, 0]	None
Waypoint-4	[0, 0, 0, 0, 0, 0, 0, 0, 0, 5]	PIR 10
Waypoint-5	[0, 0, 0, 0, 0, 0, 4, 4, 0, 0]	PIR7 dan PIR8
Waypoint-6	[0, 0, 11, 4, 0, 0, 0, 0, 0, 0]	PIR3 dan PIR4
Waypoint-7	[0, 0, 0, 0, 0, 0, 0, 0, 0, 0]	None
Waypoint-8	[0, 0, 0, 0, 0, 0, 0, 0, 0, 0]	None
Waypoint-9	[0, 0, 0, 0, 0, 0, 0, 0, 0, 0]	None
Waypoint-10	[0, 0, 0, 0, 0, 0, 0, 0, 0, 0]	None
Waypoint-11	[0, 0, 0, 0, 0, 0, 0, 0, 0, 0]	None
Waypoint-12	[0, 0, 0, 0, 0, 0, 0, 0, 0, 0]	None

From Waypoint-1 to Waypoint-3, no PIR sensors detected the victim's movement. At Waypoint-4, it can be seen that PIR1 to PIR9 did not detect the victim; however, PIR10 detected the victim's movement five times. On Waypoint-5, PIR1, 2, 3, 4, 5, 6, 9, and 10 did not detect the victim; however, PIR7 and PIR8

each detected the victim's movement four times. Then on Waypoint-6, PIR1, 2, 5, 6, 7, 8, 9, and 10 did not detect the victim; however, PIR3 and PIR4 each detected the victim's movement eleven times and four times, respectively. From Waypoint-7 to Waypoint-12, no PIR sensors detected the victim's movement. Waypoint-1, 2, 3, 7, 8, 9, 10, 11, and 12 cannot detect the victim (the victim is out-of-range from these observation points), so these data will be ignored in the triangulation process.

At Waypoint-4, PIR10 detected the victim's presence; thus, the victim is at an angle of  $342^\circ$  relative to the UAV. At Waypoint-5, PIR7 and PIR8 detected the victim's presence; thus, the victim is at an angle of  $252^\circ$  relative to the UAV. Finally, at Waypoint-6, PIR3 and PIR4 detected the victim (although PIR3 detected the victim more than PIR4, the sensor system would still assume that both PIR sensors detected the victim); thus, the victim is at an angle of  $108^\circ$  relative to the UAV. Therefore, the value of the angle relative to global reference for Waypoint-4, 5, and 6 are:

$$\begin{aligned}\theta_4 &= \theta_{UAV,4} + 90^\circ - \theta_{victim,4} = 71.276904^\circ + 90^\circ - 342^\circ = -180.723095^\circ \\ \theta_5 &= \theta_{UAV,5} + 90^\circ - \theta_{victim,5} = 63.519874^\circ + 90^\circ - 252^\circ = -98.480125^\circ \\ \theta_6 &= \theta_{UAV,6} + 90^\circ - \theta_{victim,6} = 61.343103^\circ + 90^\circ - 108^\circ = 43.343103^\circ\end{aligned}$$

The position of Waypoint-4, 5, and 6 are:

$$\begin{aligned}L_4 &= (x_4, y_4) = (99.147575, 2.386516) \\ L_5 &= (x_5, y_5) = (99.147598, 2.386493) \\ L_6 &= (x_6, y_6) = (99.147568, 2.386473)\end{aligned}$$

The system of equations generated by these data can be simplified as matrix (7) where:

$$\begin{aligned}A &= \begin{bmatrix} -\tan(-180.723095^\circ) & 1 \\ -\tan(-98.480125^\circ) & 1 \\ -\tan(43.343103^\circ) & 1 \end{bmatrix} = \begin{bmatrix} 0.012621 & 1 \\ -6.707070 & 1 \\ -0.943773 & 1 \end{bmatrix} \\ c &= [X \quad Y] \\ b &= \begin{bmatrix} 2.386516 - 99.147575 \tan(-180.723095^\circ) \\ 2.386493 - 99.147598 \tan(-98.480125^\circ) \\ 2.386473 - 99.147568 \tan(43.343103^\circ) \end{bmatrix} = \begin{bmatrix} 3.637865 \\ -662.603422 \\ -91.186395 \end{bmatrix}\end{aligned}$$

Thus the position of the victim is:

$$c = ((A^T A)^{-1} A^T b)^T = [99.147601 \quad 2.386511]$$

Table 3 compares the victim's calculated position and the victim's actual position. The victim's actual position was taken from the GPS reading of the victim's smartphone. The difference in value between the victim's calculated and actual position results in a distance of 3.094 m. This value indicates that the system could determine the victim's position with an error value below 5 m. According to the survey by the Polka *et al.* [31], an error level below 5 m is sufficient for SAR operations.

Table 3. Comparison of the triangulated victim's position with the actual victim's position

Victim's Position	Longitude	Latitude
Triangulation	99.147601	2.386511
Real Position	99.147579	2.386494
Value Difference	0.000022	0.000017

The monitoring website is shown in Figure 17. The victim's position is marked using the red marker, the observation points are marked using blue markers, and the flight path of the UAV is depicted with a yellow line. It can be seen that the victim's position is in the middle of Waypoint-4, 5, and 6. When compared to the experimental scenario picture Figure 15, the appearance of the website is in accordance with the experimental scenario; thus, the data displayed by the website is correct. We also observed that the victim's position data, total detection of each PIR sensor, the longitude and latitude position of the observation points, and the direction of the UAV at each observation point have also been appropriately stored.



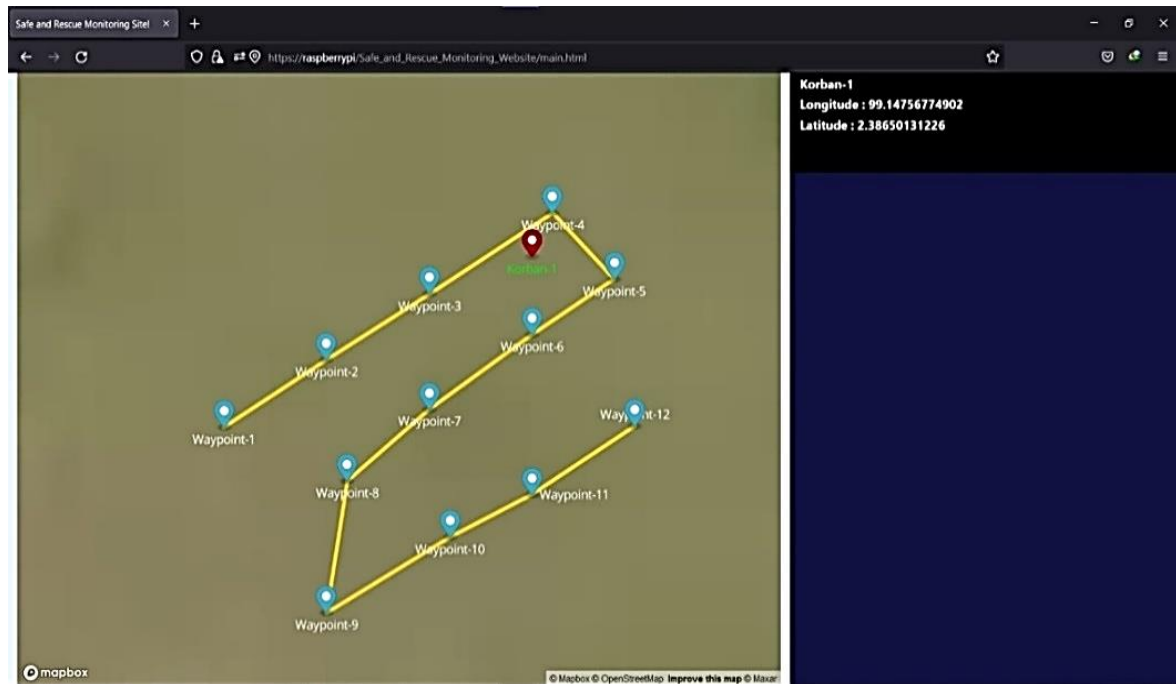


Figure 17. The monitoring website after conducting the test scenario

Table 4 compares our work and the system used in [4]–[9] in various aspects. The search range for our work was smaller than other works. Our system was proven capable of detecting a single victim; however, we have not tested its capabilities of detecting more than one victim. Our system surpassed other works in processing time, as it uses a simple sensor and algorithm. To detect victims, [4], [5], [8] relied on the operator; thus, the processing time was not specified. The accuracy of our system was also on par with other works. This comparison shows that we need to improve our system's search range and capability for detecting multiple victims.

Table 4. Comparison with the system used in [4]–[9]

System	Method	Search Range	Processing Time	Accuracy	Single/Multi-human Detection
Our work	PIRs & Triangulation	$\pm 35 \text{ m} \times 15 \text{ m}$	Immediate	$< 5 \text{ m}$	Single
[4]	Infrared Camera	Indoor	-	$< 5 \text{ m}$	Single
[5]	Camera	$3 \text{ km} \times 4 \text{ km}$	-	$< 5 \text{ m}$	Multi
[6]	Camera & Image Processing	$\pm 50 \text{ m} \times 32 \text{ m}$	250 ms	$< 5 \text{ m}$	Multi
[7]	Thermal Camera & Image Processing	$\pm 50000 \text{ m}^2$	5 minutes	$< 5 \text{ m}$	Multi
[8]	Camera	$> 5 \text{ km}$	-	$< 5 \text{ m}$	Multi
[9]	Ultra-Wide Band & Localization Method	$\pm 7.5 \text{ m} \times 7.6 \text{ m}$	Immediate	$< 5 \text{ m}$	Single

#### 4. CONCLUSION

In this research, we proposed a novel system for assisting SAR team in searching for disaster victim. The system was designed to search and determine the position of disaster victim in a fairly short time. We used PIR sensors to detect the victim's movement and the triangulation method to determine the victim's position. We also proposed a quadcopter UAV system to carry the sensor system through the disaster area. The system was tested on an experimental scenario, and the results showed that the system was able to detect and determine the position of a victim. Compared to other works', our system has an advantage in terms of processing time. Furthermore, our system's accuracy was also on par with other works. However, our system's search range and multi-human detection capability must be addressed in future works.




#### ACKNOWLEDGEMENTS

The authors of this paper would like to thank Del Institute of Technology for their financial support on this research.




## REFERENCES

- [1] D. C. Cooper, *Fundamentals of search and rescue*. Jones & Bartlett Learning, 2005.
- [2] J. Liu, Y. Wang, B. Li, and S. Ma, "Current research, key performances and future development of search and rescue robots," *Frontiers of Mechanical Engineering in China*, vol. 2, no. 4, pp. 404–416, Oct. 2007, doi: 10.1007/s11465-007-0070-2.
- [3] R. D. Arnold, H. Yamaguchi, and T. Tanaka, "Search and rescue with autonomous flying robots through behavior-based cooperative intelligence," *Journal of International Humanitarian Action*, vol. 3, no. 1, Dec. 2018, doi: 10.1186/s41018-018-0045-4.
- [4] S. Lee, D. Har, and D. Kum, "Drone-assisted disaster management: finding victims via infrared camera and Lidar sensor fusion," in *2016 3rd Asia-Pacific World Congress on Computer Science and Engineering (APWC on CSE)*, Dec. 2016, pp. 84–89, doi: 10.1109/APWC-on-CSE.2016.025.
- [5] D. Erdos, A. Erdos, and S. E. Watkins, "An experimental UAV system for search and rescue challenge," *IEEE Aerospace and Electronic Systems Magazine*, vol. 28, no. 5, pp. 32–37, May 2013, doi: 10.1109/MAES.2013.6516147.
- [6] M. T. Agcayazi, E. Cawi, A. Jurgenson, P. Ghassemi, and G. Cook, "ResQuad: Toward a semi-autonomous wilderness search and rescue unmanned aerial system," in *2016 International Conference on Unmanned Aircraft Systems (ICUAS)*, Jun. 2016, pp. 898–904, doi: 10.1109/ICUAS.2016.7502618.
- [7] D. S. López, "Micro aerial vehicles (MAV) assured navigation in search and rescue missions robust localization, mapping and detection," Escola Tècnica Superior d'Enginyeria Industrial de Barcelona, 2015.
- [8] L. Auer, A. Feichtner, C. Oberauer, and F. Steinhäusler, "EU CURSOR drone fleet: Fast and cost-effective rescue of victims buried under rubble," *International Research Journal of Engineering and Technology (IRJET)*, vol. 7, no. 6, pp. 6870–6877, 2020.
- [9] T. Kobayashi *et al.*, "Wireless technologies to assist search and localization of victims of wide-scale natural disasters by unmanned aerial vehicles," in *2017 20th International Symposium on Wireless Personal Multimedia Communications (WPMC)*, Dec. 2017, pp. 404–410, doi: 10.1109/WPMC.2017.8301846.
- [10] R. Hahn, D. Lang, M. Haselich, and D. Paulus, "Heat mapping for improved victim detection," in *2011 IEEE International Symposium on Safety, Security, and Rescue Robotics*, Nov. 2011, pp. 116–121, doi: 10.1109/SSRR.2011.6106769.
- [11] Y. Liu *et al.*, "The design of a fully autonomous robot system for urban search and rescue," in *2016 IEEE International Conference on Information and Automation (ICIA)*, Aug. 2016, pp. 1206–1211, doi: 10.1109/ICInfA.2016.7832003.
- [12] I. I. Mohamed, L. Lim, Kun, and N. E. Mohamed, "An embedded autonomous search and rescue mobile robotic system for alive human detection," *International Journal of Modern Trends in Engineering and Research (IJMTER)*, vol. 7, no. 4, pp. 22–29, 2020, doi: 10.21884/IJMTER.2020.7022.0CLWX.
- [13] T. Teixeira, G. Dublon, and A. Savvides, "A survey of human-sensing: methods for detecting Presence, count, Location, track, and identity," *ACM Computing Surveys*, vol. 5, no. 1, 2010.
- [14] J. Xiao, Z. Zhou, Y. Yi, and L. M. Ni, "A survey on wireless indoor localization from the device perspective," *ACM Computing Surveys*, vol. 49, no. 2, pp. 1–31, Nov. 2016, doi: 10.1145/2933232.
- [15] T. Murray and S. F. Hasan, "Present state of the art in post disaster victim localization," in *2020 IEEE 5th International Symposium on Telecommunication Technologies (ISTT)*, Nov. 2020, pp. 51–56, doi: 10.1109/ISTT50966.2020.9279342.
- [16] C.-M. Wu, X.-Y. Chen, C.-Y. Wen, and W. A. Sethares, "Cooperative networked PIR detection system for indoor human localization," *Sensors*, vol. 21, no. 18, Sep. 2021, doi: 10.3390/s21186180.
- [17] A. Industries, "PIR motion sensor." New York, 2021.
- [18] S. Narayana, R. V. Prasad, V. S. Rao, T. V. Prabhakar, S. S. Kowshik, and M. S. Iyer, "PIR sensors: Characterization and novel localization technique," in *Proceedings of the 14th International Conference on Information Processing in Sensor Networks*, Apr. 2015, pp. 142–153, doi: 10.1145/2737095.2742561.
- [19] Y. Yuebin, F. Guodong, G. Xuemei, and W. Guoli, "Compressed infrared bearing sensor for human localization: Design and implementation," in *2012 IEEE International Conference on Information and Automation*, Jun. 2012, pp. 936–940, doi: 10.1109/ICInfA.2012.6246950.
- [20] K.-C. Lai, B.-H. Ku, and C.-Y. Wen, "Using cooperative PIR sensing for human indoor localization," in *2018 27th Wireless and Optical Communication Conference (WOCC)*, Apr. 2018, pp. 1–5, doi: 10.1109/WOCC.2018.8372703.
- [21] S. Lee, K. Ha, and K. Lee, "A pyroelectric infrared sensor-based indoor location-aware system for the smart home," *IEEE Transactions on Consumer Electronics*, vol. 52, no. 4, pp. 1311–1317, Nov. 2006, doi: 10.1109/TCE.2006.273150.
- [22] Zhiqiang Zhang, Xuebin Gao, Jit Biswas, and Jian Kang Wu, "Moving targets detection and localization in passive infrared sensor networks," in *2007 10th International Conference on Information Fusion*, 2007, pp. 1–6, doi: 10.1109/ICIF.2007.4408178.
- [23] X. Liu, T. Yang, S. Tang, P. Guo, and J. Niu, "From relative azimuth to absolute location," in *Proceedings of the 26th Annual International Conference on Mobile Computing and Networking*, Apr. 2020, pp. 1–14, doi: 10.1145/3372224.3380878.
- [24] E. Lygouras, A. Gasteratos, K. Tarchanidis, and A. Mitropoulos, "ROLFER: A fully autonomous aerial rescue support system," *Microprocessors and Microsystems*, vol. 61, pp. 32–42, Sep. 2018, doi: 10.1016/j.micpro.2018.05.014.
- [25] G. Ononiwu, A. Okoye, J. Onojo, and N. Onuekwusi, "Design and implementation of a real time wireless quadcopter for rescue operations," *American Journal of Engineering Research (AJER)*, vol. 5, no. 9, pp. 130–138, 2016.
- [26] M. F. Ahmed, M. N. Zafar, and J. C. Mohanta, "Modeling and analysis of quadcopter F450 frame," in *2020 International Conference on Contemporary Computing and Applications (IC3A)*, Feb. 2020, pp. 196–201, doi: 10.1109/IC3A48958.2020.233296.
- [27] W.-H. Liao, Y. Kao, and Y.-S. Li, "A sensor deployment approach using glowworm swarm optimization algorithm in wireless sensor networks," *Expert Systems with Applications*, vol. 38, no. 10, pp. 12180–12188, Sep. 2011, doi: 10.1016/j.eswa.2011.03.053.
- [28] D. Agbissoh OTOTE *et al.*, "A decision-making algorithm for maritime search and rescue plan," *Sustainability*, vol. 11, no. 7, Apr. 2019, doi: 10.3390/su11072084.
- [29] D. Zhang, F. Xia, Z. Yang, L. Yao, and W. Zhao, "Localization technologies for indoor human tracking," in *2010 5th International Conference on Future Information Technology*, 2010, pp. 1–6, doi: 10.1109/FUTURETECH.2010.5482731.
- [30] P. Kułakowski, J. Vales-Alonso, E. Egea-López, W. Ludwin, and J. García-Haro, "Angle-of-arrival localization based on antenna arrays for wireless sensor networks," *Computers & Electrical Engineering*, vol. 36, no. 6, pp. 1181–1186, Nov. 2010, doi: 10.1016/j.compeleceng.2010.03.007.
- [31] M. Półka, S. Ptak, and L. Kuziora, "The use of UAV's for search and rescue operations," *Procedia Engineering*, vol. 192, pp. 748–752, 2017, doi: 10.1016/j.proeng.2017.06.129.




**BIOGRAPHIES OF AUTHORS**

**Fajar Sam Hutabarat**    is a Bachelor of Electrical Engineering at Del Institute of Technology. He has some interest at automation, robotics, websites, artificial intelligence, and industrial Internet of things. He can be contacted at [els18017@students.del.ac.id](mailto:els18017@students.del.ac.id).






**Imanuel Maurice Darmawan Sitanggang**    is a Bachelor of Electrical Engineering at Del Institute of Technology. He has some interest at automation, electronics, and industrial Internet of things. He can be contacted at [els18019@students.del.ac.id](mailto:els18019@students.del.ac.id).






**Damanik, Joy Andrew Immanuel**    is a Bachelor of Electrical Engineering at Del Institute of Technology. He likes to study physics, electronics, and robotics. He can be contacted at [els18027@students.del.ac.id](mailto:els18027@students.del.ac.id).



**Guntur Petrus Boy Knight**    is graduated with a bachelor's degree from Telecommunication Engineering ITB in 2012. Completed the master's Program in 2018 in the field of Electrical Engineering. Currently, he is the head of ITdel's Electrical Engineering Study Program. He is actively conducting research in the field of unmanned aerial vehicle and wireless communication system. He can be contacted at [guntur\\_petrus@students.itb.ac.id](mailto:guntur_petrus@students.itb.ac.id).



**Albert Sagala**    is a senior lecturer in the Department of Electrical Engineering, Del Institute of Technology. He graduated from the Bachelor of Engineering Physics Program (ITB), Master of Instrumentations and Control (ITB). He is currently doing a lot of research in the area of smart farming, wireless sensor networks, internet of things and cyber security. Currently, he also serves as chairman of the research and community service institute at ITdel. He can be contacted at [albert@del.ac.id](mailto:albert@del.ac.id).